Ligand Effects on the Fluorescence Properties of Tyrosine-9 in Alpha 1-1 Glutathione *S*-Transferase†

Eric C. Dietze,‡ Regina W. Wang,§ Anthony Y. H. Lu,§ and William M. Atkins*,‡

University of Washington, Medicinal Chemistry, Box 357610, Seattle, Washington 98195-7610, and Department of Drug Metabolism, Merck Research Laboratories, Box 2000, Rahway, New Jersey 07065

Received December 21, 1995; Revised Manuscript Received March 15, 1996⊗

ABSTRACT: A conserved tyrosine plays a critical role in catalysis by mammalian glutathione *S*-transferases (GSTs) of the alpha-, mu-, and pi-classes, by forming a hydrogen bond to and stabilizing the thiolate form of glutathione. The hydrogen bonding properties of this tyrosine in the rat A1-1 GST (Tyr-9), in the absence and presence of ligands, have been studied by steady state and time-resolved fluorescence spectroscopy. In order to achieve this, the single tryptophan (Trp 21) found in the rat A1-1 GST has been replaced with the fluorometrically silent phenylalanine (W21F). Additionally, a double mutant lacking this tryptophan and the catalytic tyrosine (W21F:Y9F) has been constructed, and these mutants have been used as probes of ligand effects at Tyr-9. A comparison of the correlated excitation−emission spectra of the W21F mutant and the W21F-Y9F indicates that a red-shifted emission component is contributed by Tyr-9 with excitation bands at 255 and 300 nm, in the ligand-free enzyme. The pH-dependence of the intensity of these spectral cross-peaks is consistent with an active site tyrosine with a pK_a of 8.1−8.3. Upon addition of GSH, the red-shifted component is quenched. Multifrequency phase/modulation fluorescence experiments qualitatively demonstrate that GSH causes a decrease in the average excited state lifetime on the red-edge of the spectrum of W21F but not of the W21F:Y9F spectrum. Steady state correlated difference spectra (W21F − W21F:Y9F) have been used to obtain a model for the excitation−emission correlated spectrum of Tyr-9, which indicates that Tyr-9 is heterogeneous at pH 7.5, with properties of both tyrosinate and "normal tyrosine". The tyrosinate fraction is eliminated, and the blue-shifted component becomes more intense upon addition of GSH conjugates, indicating that the weak hydrogen bond between Tyr-9 and thioethers has little charge-transfer character. The *S*-methyl GSH yields an "anomalous" spectrum at pH 7.5, which retains cross-peaks consistent with ionized tyrosinate. These results indicate that, in the absence of ligand, Tyr-9 forms a strongly polarized hydrogen bond or a fraction of the phenolic hydroxyl group is partially deprotonated. However, when a GSH conjugate with a sufficiently large hydrophobic group occupies the H-site, Tyr-9 is fully protonated, with little charge-transfer character.

The glutathione *S*-transferases (GSTs)[1] catalyze the nucleophilic attack of glutathione (GSH) on numerous lipophilic electrophiles (Rushmore & Pickett, 1993; Mannervik & Danielson, 1988; Armstrong, 1991). These reactions play a critical role in the detoxication of carcinogens, drugs, and the metabolism of endogenous compounds. The mammalian cytosolic GSTs are represented by four gene classes, which are designated alpha, pi, mu, and theta (Ketterer & Christodoulides, 1994). The primary amino acid sequence homologies between proteins from different gene classes range from only 25% to 35%, yet X-ray crystallographic data from alpha-, pi-, and mu-class GSTs indicate that they share similar overall folding topologies [see Dirr et al. (1994) for review of structures].

GSTs from each of these gene classes clearly provide a GSH binding site within the N-terminal one-third of the proteins and a hydrophobic binding site (H-site) for electrophiles. The hydrophobic sites are composed of residues from this N-terminal portion of the protein and from the remaining C-terminal portion. One active site feature which is completely conserved in the alpha-, pi-, and mu-class enzymes is a hydrogen bond between the thiol of bound GSH and the phenolic hydroxyl group of a tyrosine side chain. The importance of this hydrogen bond in GST catalysis is clear, based on studies with site-directed mutants (Liu et al., 1992; Wang et al., 1992a; Kong et al., 1992). In addition, spectroscopic experiments have indicated that the pK_a of the thiol of GSH is lowered from ∼9.3 in solution to 6.5−6.9 at the active site of GSTs, and that the thiolate anion, GS^-, is the predominant speces when bound to the protein at physiological pH (Graminski et al., 1989). From these results, the detailed structure of this hydrogen bond has been inferred as Tyr-OH···$^-$SG, with the shared proton residing completely on the hydroxyl group.

However, biochemical evidence suggests that the active site tyrosine has significant nucleophilic character, rendering it reactive toward diethyl pyrocarbonate (even in the presence of GSH; Meyer et al., 1993) and 2-(*S*-glutathionyl)-3,5,6-trichlorobenzoquinone (Ploemen et al., 1994). Furthermore,

† This work was supported by the National Institutes of Health (GM51210-01A1).

* Corresponding author. Tel: (206) 685-0379. FAX: (206) 685-3252. E-mail: winky@u.washington.edu.

‡ University of Washington.

§ Merck Research Laboratories.

⊗ Abstract published in *Advance ACS Abstracts,* May 1, 1996.

[1] Abbreviations: GSH, glutathione; GST, glutathione *S*-transferase; GS^-, the thiolate form of GSH; SDS−PAGE, sodium dodecyl sulfate−polyacrylamide gel electrophoresis; Hepes, *N*-(2-hydroxyethyl)piperazine-*N*′-2-ethanesulfonic acid; Mes, 2-(*N*-morpholino)ethanesulfonic acid; Tyr-9-O^-, the phenolate anion of Tyr-9.

S0006-2960(95)03034-0 CCC: $12.00

fluorescence titration of an alpha-class isozyme (Atkins et al., 1993), UV−visible spectroscopic data (Bjornestedt et al., 1995), and the chemical modification studies and electrostatic calculations with a pi-class GST (Meyer et al., 1993; Karshikoff et al., 1993) indicate that, in the absence of GSH, as much as 25% of the active site tyrosine exists as the unprotonated tyrosinate. These data suggest that this catalytically important residue possesses a significant degree of anionic character (Tyr-$O^{-\delta}\cdots{}^{+\delta}H$) in both substrate-free and GSH-bound states. Thus, a detailed picture of the hydrogen bond between GS^- and the active site tyrosine remains obscure, and the position of the shared proton in various ligand states has not been established. The possibility that this hydrogen bond has "symmetrical" character, as in Tyr-$O^{-\delta}\cdots{}^{+\delta}H\cdots{}^{-}SG$, has been suggested (Meyer et al., 1993; Ji et al., 1992).

In addition, the dielectric environment and the extent of solvation of this hydrogen bond are likely to affect the rates of reaction with hydrophobic electrophiles bound at the "H-site". The magnitude of solvent kinetic isotope effects supports this hypothesis (Huskey et al., 1991). Indeed, the X-ray structure of the mu-class and the pi-class binary complexes, GST·GS^-, indicate that the thiolate and the tyrosine hydroxyl form a partially solvated hydrogen bond (Dirr et al., 1994; Ji et al., 1992). In contrast, structurally defined water molecules which solvate the Tyr-OH are not observed in the presence of *S*-hexyl GSH or *S*-benzyl GSH, and the hydrogen bond to glutathione conjugates is apparently not solvated (Sinning et al., 1993). Thus, it is likely that various hydrophobic substrates displace water from the H-site to varying degrees. Notably, in the absence of ligands, the active site tyrosine of the human A1-1 GST is hydrated by a disordered water molecule, and it remains within hydrogen-bonding distance of the amide backbone nitrogen of Arg-15 (Cameron et al., 1995).

In order to further characterize the environment of this tyrosine and the extent to which various ligands modulate its relative solvation, we have used in our studies the fluorescence properties of Tyr-9 in the rat A1-1 GST. The fluorescence emission of tyrosine side chains is remarkably sensitive to the hydrogen-bonding environment, and it has been established that the extent of charge-transfer in a hydrogen-bonded complex is dependent on the basicity of the acceptor and on the solvent polarity (Ratajczak, 1972; Willis & Szabo, 1991). Here we extend our previous studies (Atkins et al., 1993) with the engineered rat alpha 1-1 GSTs, W21F and W21F:Y9F, which contain no tryptophans. Together these mutants allow for characterization of the local environment of Tyr-9 in the presence of various ligands. A novel combination of steady state fluorescence properties, difference emission spectra, and ligand quenching has been used to selectively characterize Tyr-9. Correlated excitation−emission spectra indicate that the Tyr-9 is either strongly hydrogen bonded to a basic acceptor in the substrate-free GST or that it is partially deprotonated. Furthermore, the extent of charge-transfer in the hydrogen-bonded Tyr-9 changes differentially when various GSH conjugates are bound to GST.

MATERIALS AND METHODS

Site-Directed Mutagenesis. Site-directed mutants were obtained as previously described (Wang et al., 1991).

Protein Purification. Mutant GSTs were purified as described previously (Wang et al., 1989), with the following modifications, which were found to be necessary to obtain electrophoretically pure enzyme. The fractions eluted from the *S*-hexyl GSH column which contained GST activity were pooled, and ligand was removed by gel filtration on a Sephadex G-25 column equilibrated with buffer A (7 mM potassium phosphate, 2 mM EDTA, pH 6.9). The GST was then chromatographed on a CM-cellulose column equilibrated with buffer A. The fractions which contained GST were loaded, and the CM-cellulose column was washed with 5 column volumes of buffer A. The GST was then eluted with 5 column volumes of 50% buffer A/50% 250 mM potassium phosphate (pH 6.7). The fractions that contained GST activity were concentrated and stored at −20 °C for future use. Mutant proteins purified by this method were greater than 97% pure, on the basis of SDS−PAGE analysis.

Steady State Fluorescence. Steady state fluorescence measurements were performed on a SLM-Aminco 8100C fluorimeter thermostated at 5 °C. All slit widths were 2 mm in the excitation channel and 8 and 4 mm in the emission channel. Samples were 0.25 μM GST in 50 mM Hepes-Mes at pHs indicated throughout or 50 mM Capso for pH 9.5 and were stirred throughout the data acquisition. Appropriate buffer "blanks" were subtracted from all spectra. When present, ligand concentrations were 1.25 mM. After addition of ligand, samples were equilibrated in the cuvette for 2 min prior to data acquisition. It was demonstrated experimentally that this concentration of GSH or *S*-methyl GSH was sufficient to saturate the enzyme. Because the other ligands used in these studies have been shown to bind more tightly than GSH to alpha-class GSTs (Askeolf et al., 1975), we assume that the other ligands are also saturating at this concentration. The excitation wavelengths used for correlated spectra were at 5 nm intervals, starting at 245 nm and ending at 305 nm. The emission wavelength range was 305−400 nm. Each spectrum was corrected for the wavelength dependence of the lamp output. Difference emission spectra are the average of four separate difference spectra. The spectral center of mass, v_i, was calculated as $v_i = \sum v_i(I)/\sum v_i$, where I is the emission intensity at wavelength v_i. The center of mass represents the average energy of emission.

Phase/Modulation Fluorescence. Multifrequency phase and modulation experiments were performed at the Laboratory for Fluorescence Dynamics (LFD) at the University of Illinois, Urbana, IL. Samples were 10 μm W21F or W21F:Y9F in 50 mM Hepes-Mes, pH 7.5. Excitation at 290 nm was achieved with a frequency-doubled, mode-locked Nd:YAG laser synchronously pumping a cavity-dumped rhodamine 6G dye laser (Coherent Corp., Palo Alto, CA). Emission was detected with band pass filters (8 nm band pass). Intensity decay measurements employed polarizers in the excitation and emission channels, with orientations offset at 55°. The precision of the phase angle and modulation ratio measurements was $<0.6°$ and <0.004, respectively. The decay data were analyzed with the multivariable fitting program, Globals Unlimited, which utilizes a Marquardt−Levenberg nonlinear least-squares analysis, as described in detail previously (Knutson et al., 1983; Beechem et al., 1991). Decay data were fitted to a sum of exponentals model. Attempts to fit the data to models describing continuous distribution of decay parameters did not improve the "fits".

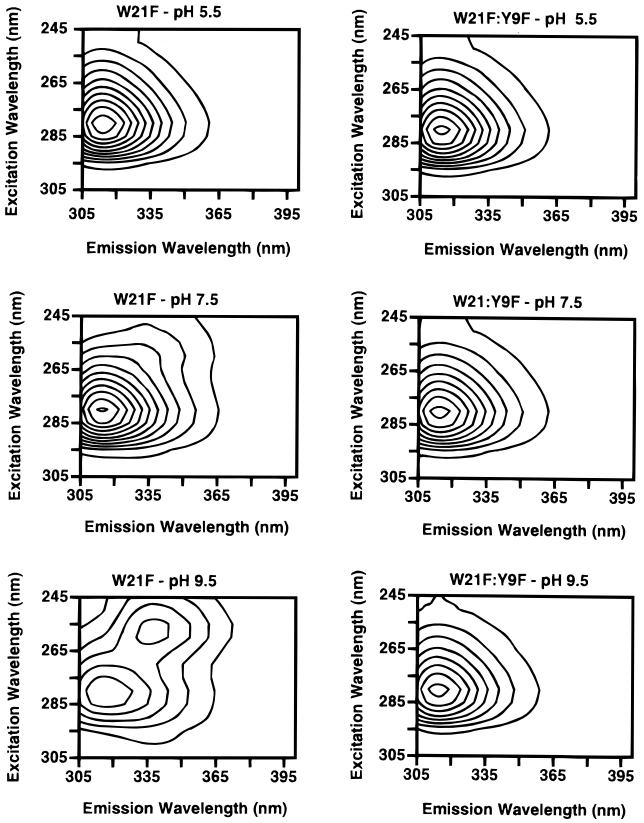

FIGURE 1: Excitation−emission correlated spectral contours for W21F and W21F:Y9F at several pHs. Tyr-9 provides a spectral component with emission at 340 nm and excitation at 255 and 305 nm, which increases in intensity with increasing pH.

RESULTS

Substrate-Free and GSH-Bound Glutathione S-Transferase. We have described previously the mutant rat A1-1 GST proteins W21F and W21F:Y9F, in which the single tryptophan found in the wild protein has been replaced with the fluorimetrically silent phenylalanine (Atkins et al, 1993). In addition, the W21F:Y9F mutant has a phenylalanine substituted for the active site Tyr-9. Replacement of Trp-21 with phenylalanine has negligible effect on the catalytic properties of the enzyme (Wang et al., 1992b). Together, these proteins allow for the characterization of the active site tyrosine (Atkins et al., 1993). The previous characterization was specifically aimed at determining the pK_a of Tyr-9. Here the characterization is extended, in order investigate the environment of the hydrogen bond to Tyr-9, and the complete excitation−emission correlated spectral contours are shown for both proteins, at several pH values. Direct comparison of the correlated excitation−emission spectra of the ligand-free W21F and the W21F:Y9F mutant proteins indicates that, at pH 7.5, the single mutant has a strong emission "cross-peak" centered at 335−340 nm, coupled to an excitation band at ∼255 nm and a much less intense excitation band at ∼300 nm, which appears as a "lobe" on the long-wavelength side of the peak at 280 nm along the excitation axis; both of these cross-peaks are due apparently to a contribution from Tyr-9, because they are absent in the correlated contours of the W21F:Y9F protein (Figure 1). Because the emission maximum of tyrosine that is hydrogen bonded to "bulk" water (305−310 nm) is insensitive to changes in the dielectric constant of the environment [Willis and Szabo (1991) and data not shown], we propose that the cross-peaks in the correlated spectrum of the W21F mutant

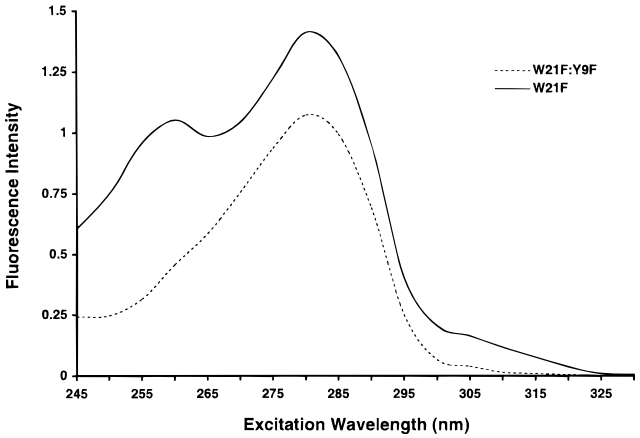

FIGURE 2: Individual excitation spectra of W21F (—) and W21F:Y9F (- - -). Emission wavelength was 350 nm. The spectra represent "slices" through the surfaces in Figure 1 at emission = 350 nm. Tyr-9 contributes the red-shifted emission component.

arise because Tyr-9 is partially deprotonated at pH 7.5 (Atkins et al., 1993), in the absence of GSH. This is based on the well-established absorbance and emission properties of tyrosine. Tyrosine absorbs maximally at ∼225 nm (ϵ = 8200 M^{-1} cm^{-1}) and at ∼278 nm (ϵ = 1350 M^{-1} cm^{-1}), and new absorbance bands are generated when the phenolic hydroxyl group is hydrogen bonded or ionized (Beaven & Holiday, 1952; Wetlaufer, 1962). Strongly hydrogen-bonded tyrosine and tyrosinate absorb maximally at ∼295 nm (ϵ = 2350 M^{-1} cm^{-1}) and ∼245−255 nm (ϵ = 11 000 M^{-1} cm^{-1}). The observed "cross-peaks" in the 2D contour plot of the W21F mutant are much more intense at pH 9.5 and completely absent at pH 5.5 (Figure 1), as expected for a change in the ionization state of Tyr-9 with a pK_a of 8.1−8.3, as measured by UV spectroscopy and fluorescence (Atkins et al., 1993; Bjornestedt et al., 1995). Individual excitation spectra (emission = 350 nm) also are shown for the two proteins at pH 7.5 in Figure 2. These spectra clearly demonstrate a red-shifted emission component arising from Tyr-9, which has unique excitation bands. The spectrum of the W21F mutant has excitation bands centered at 257 and 305 nm, which are absent in the W21F:Y9F protein. These spectra represent vertical "slices" through the 2D contour plots, at an emission wavelength 350 nm, as viewed along the excitation wavelength axis.

It has been appreciated that it is difficult to distinguish between tyrosinate, with a formal negative charge, and strongly hydrogen-bonded tyrosine, and partial charge-transfer (Ross et al., 1992). Intuitively, it is reasonable to propose that tyrosinate provides the cross-peaks which are observed for the W21F protein, rather than hydrogen-bonded tyrosine, because the recently published X-ray structure of the human A1-1 GST indicates that the only hydrogen-bonding partners within proximity to the phenolic hydroxyl group of Tyr-9 are the backbone amide of Arg-15 and a disordered water molecule (Cameron et al., 1995). The possibility that this water acts as a strong hydrogen bond acceptor is explored in the Discussion.

The possibility that Tyr-9 was hydrogen bonded to a buffer component in the absence of ligand was also considered. Free tyrosine and *N*-acetyltyrosine in solution will form hydrogen bonds with phosphate, imidazole, and other commonly used buffers (Ross et al., 1992; Willis & Szabo, 1991). Thus, it was reasonable to postulate that a buffer salt provided a good hydrogen bond acceptor for Tyr-9. However, varying

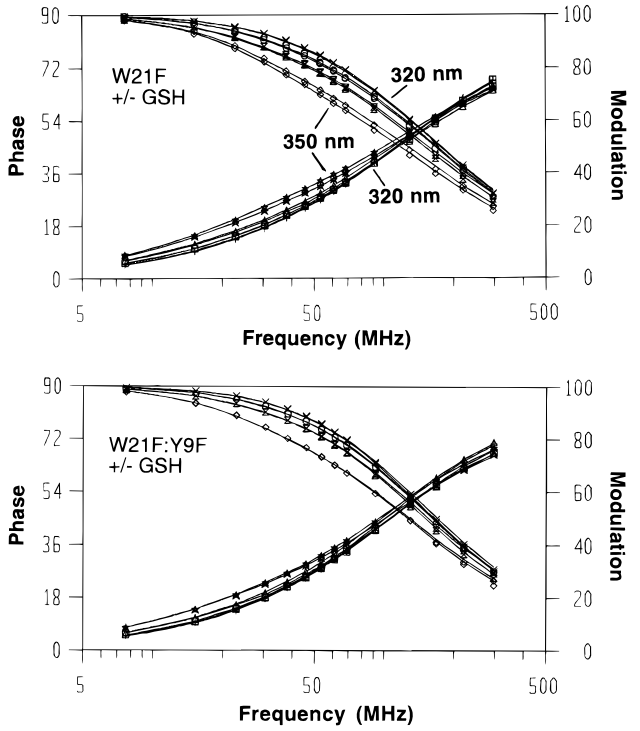

FIGURE 3: Phase modulation data for W21F and W21F:Y9F. Phase angles (phase) and modulation ratios (mod) at four emission wavelengths in the presence and absence of GSH. Phase angles: crosses, 320 nm; open squares, 330 nm; open triangles, 340 nm; stars, 350 nm. Modulation ratios: ×, 320 nm; open circles, 330 nm; hourglass, 340 nm; open diamonds, 350 nm. For the W21F:Y9F mutant GSH has no effect on the decay parameters. For W21F, GSH induces a shorter average excited state lifetime at the longer wavelengths (Table 1).

concentration of the buffer salts used here (Hepes-Mes) between 10 and 200 mM at constant pH had no effect on the steady state emission spectra of either mutant protein. Moreover, emission spectra of *N*-acetyltyrosine in solutions of these buffers did not include red-shifted components compared to *N*-acetyltyrosine in water alone (not shown). Together, these observations indicate that the unique spectral component of the W21F mutant is not due to a hydrogen bond between Tyr-9 and a buffer component.

Although the excitation spectra indicate that the Tyr-9 has unique ground state features, it was possible, in principle, that the unique cross-peaks in the correlated spectra of the W21F mutant were due to fluorescence of tyrosinate formed during the excited state. It is well established that the pK_a of tyrosine decreases from ~10.3 to ~3.5 upon reaching the first excited singlet state (Rayner et al., 1978). In particular, it was necessary to consider the possibility that a proton was transferred during the excited state from Tyr-9 to a protein-derived base in the absence of ligand or to GS^- when this cofactor is bound. These possibilities were examined with multifrequency phase/modulation experiments.

The frequency responses of the W21F and the W21F:Y9F mutant properties were determined in the presence and absence of GSH, at pH 7.5 (Figure 3). Global Analysis of the phase and modulation data afforded three excited state lifetimes at four emission wavelengths spanning the long-wavelength side of the total protein emission spectra (Table 1). The data indicate clearly that GSH had little effect on the excited state decay parameters of the W21F:Y9F at any wavelength, or on the W21F protein, at 320 nm (Figure 3). The phase and modulation curves are essentially superimposable at each wavelength for the double mutant. The data are also nearly superimposable at each wavelength for the double mutant. The data are also nearly superimposable for the W21F mutant at the shorter wavelengths. However, at the red-edge of the emission spectrum, GSH shifts the frequency response of the W21F mutant, and the data for the W21F in the presence and absence of GSH become easily distinguishable. This further demonstrates that the red-shifted emission component is due to Tyr-9. Quenching of tyrosine by sulfhydryl groups is well documented (Cogwill, 1976; Ross et al., 1992). The decrease in average excited state lifetime following GSH binding suggests that a dynamic quenching mechanism is, at least partially, operative (Eftink, 1991). It is impossible to determine from these experiments whether a static quenching mechanism also contributes.

Table 1: Global Analysis of Phase/Modulation Data[a]

	lifetime (ns), (fractional intensity)			
	emission wavelength			
protein/ligand	320 nm	330 nm	340 nm	350 nm
W21F	3.45 (0.22)	4.08 (0.23)	5.14 (0.27)	5.35 (0.38)
	1.25 (0.76)	1.24 (0.74)	1.30 (0.70)	1.26 (0.58)
	0.45 (0.02)	0.49 (0.03)	0.50 (0.03)	0.45 (0.12)
	avg = 1.73	avg = 1.89	avg = 2.46	avg = 2.84
W21F + GSH	3.61 (0.21)	4.12 (0.24)	5.23 (0.18)	5.21 (0.30)
	1.40 (0.76)	1.41 (0.75)	1.45 (0.70)	1.41 (0.53)
	0.47 (0.03)	0.38 (0.01)	0.45 (0.12)	0.40 (0.17)
	avg = 1.82	avg = 2.03	avg = 2.00	avg = 2.36
W21F:Y9F	3.51 (0.15)	4.09 (0.13)	6.25 (0.14)	6.23 (0.30)
	1.44 (0.83)	1.48 (0.85)	1.61 (0.79)	1.52 (0.65)
	0.39 (0.02)	0.40 (0.02)	0.48 (0.07)	0.33 (0.05)
	avg = 1.82	avg = 1.80	avg = 2.18	avg = 2.87
W21F:Y9F + GSH	3.91 (0.11)	4.59 (0.14)	6.51 (0.14)	6.38 (0.29)
	1.50 (0.08)	1.50 (0.84)	1.63 (0.81)	1.56 (0.67)
	0.37 (0.01)	0.36 (0.02)	0.49 (0.05)	0.39 (0.04)
	avg = 1.75	avg = 1.91	avg = 2.25	avg = 2.91

[a] Conditions as described in Materials and Methods. Precision of individual lifetime values is ±0.004 ns. The reported average values are weighted averages based on the fractional intensities.

In addition, these experiments provided critical information about the decay process. The excited state decay data indicate that the red-shifted emission of W21F was not due to an excited state proton transfer from Tyr-9 which subsequently affords a fluorescent tyrosinate. When excited state decay processes occur, sharp changes in the decay parameters with changes in emission or excitation wavelength are expected, corresponding to two states of the excited state reaction (Ross et al., 1992; Willis & Szabo, 1991). In addition, negative pre-exponential factors are recovered when excited state reactions dominate the decay pathway. Neither of these diagnostic fluorescence properties was observed in any of the data fitting we attempted. Furthermore, the Globals Unlimited analysis software used for data fitting allows for testing models which include an excited state reaction. An explicit search for excited state reactions resulted in poor correspondence between the mathematical models and the data obtained for W21F in either the ligand-free or GSH-bound states ($\chi^2 > 6$, not shown). On the basis of the decay data and these modeling efforts, excited state reactions do not make a significant contribution to the tyrosine fluorescence observed in the rat A1-1 mutant GSTs, in the presence or absence of GSH. On the basis of results reported by Willis and Szabo (1991) and others (Ross et al., 1991), this is not surprising. Briefly, it has been demonstrated that excited state transfer of the proton from the

phenolic oxygen of tyrosine to a strong hydrogen bond acceptor is extremely unlikely due to excited state relaxation rates that are fast relative to proton transfer. The phase/modulation data, therefore, indicate that the red-shifted emission correlated to excitation bands at 255 and 305 nm results from unique ground state properties of the active site tyrosine, Tyr-9, rather than excited state deprotonation.

It should be stressed that, due to spectral overlap with other tyrosines contained in the protein, these data do not allow for deconvolution of a decay-associated spectrum of Tyr-9 (Beechem et al., 1991) or assignment of specific lifetime components uniquely to Tyr-9. In fact, the reproducible GSH-induced spectral changes are small, and when models are compared in which only the lifetimes change or only the fractional intensities change, "fits" of the data to different models are statistically equivalent. Therefore, a detailed physical model for the excited state decay of Tyr-9 was not obtained. This was not the goal of these experiments, and further comparison of different possible linkage schemes with Global Analysis was not performed. Rather, these data demonstrate that excited state deprotonation of Tyr-9 is unlikely.

Difference Spectra. In principle, difference emission spectra (W21F − W21F:Y9F) will afford qualitative model spectra of Tyr-9, assuming insignificant structural change upon substitution of Tyr-9. The W21F:Y9F is presumed to be structurally intact, because it retains completely its affinity for the *S*-hexyl GSH-agarose column. Furthermore, the X-ray structure of the binary complex of the corresponding Y6F mutant of the M3-3 GST, with GSH bound, is not significantly altered compared to the wild type (Liu et al., 1992). Thus, structural perturbation is not expected to limit the use of difference spectra in this case. However, difference spectra will provide useful models of the Tyr-9 properties only when energy transfer between Tyr-9 and phenylalanines or other Tyr residues is minimal. Obviously, Tyr−Trp energy transfer is not possible in these engineered mutant proteins, and energy transfer from phenylalanines is usually inefficient, particularly at some of the longer excitation wavelengths used here (>295 nm). Moreover, the alpha-class 1-1 GST is naturally suited for minimal energy transfer between Tyr-9 and other tyrosines. The X-ray structure of the human alpha-class 1-1 GST (Sinning et al., 1993; Cameron et al., 1995) was examined for possible interactions between Tyr-9 and other tyrosines. Each of the tyrosines contained within the rat A1-1 enzyme used here is present in the human A1-1 enzyme (the human A1-1 isozyme has two additional tyrosines, Tyr-49 and Tyr-165). The shortest distances between side chain carbon atoms of Tyr-9 of one subunit (arbitrarily chosen as subunit B) and other tyrosines in each of the subunits are summarized in Table 2, along with the dihedral angles between aromatic rings. Two of the tyrosines in the human A1-1 GST which are closest to Tyr-9.

Tyr-166 and Tyr-74 in the same subunit, are not oriented well for energy transfer with Tyr-9 and therefore are unlikely to provide energy transfer partners for Tyr-9. Tyr-132 of the adjacent subunit is close enough to Tyr-9 to expect some energy transfer, assuming a Forster distance of 8−14 Å (Wu et al., 1994; Eisinger et al., 1969), and the orientation may be favorable, on the basis of the data presented below and in Table 2. The optimal dihedral angle for energy transfer between tyrosine residues is ±180 ° or when the aromatic rings are coplanar with oppositely oriented transition dipole moments (Eisinger et al., 1969). Indeed, some energy transfer from Tyr-9 to Tyr-132 may take place. However, Tyr-9 is not an efficient energy transfer acceptor, on the basis of the lack of negative pre-exponential factors for the excited state decay at longer wavelengths. From this comparison of the location of tyrosine residues in the human A1-1 GST and the rat isozyme used here, the only tyrosine which is likely to interact with Tyr-9 of the W21F mutant is Tyr-132. The data presented below indicate that, even if some energy transfer occurs, it does not eliminate the utility of the difference spectra obtained. Because the effects of pH changes and ligands on the spectra of the W21F mutant are the same as the effects on the difference spectra (see below), it is reasonable to assume that energy transfer involving Tyr-9 does not dominate the fluorescence properties of this residue.

Table 2: Distances and Angles between Tyr-9 and Other Tyrosines in Human A1-1 GST[a]

Tyr no.	distance (Å)	dihedral angle (deg)
9B−166B	11.8	−11.6
9B−49B[b]	14.0	172.2
9B−132A	15.2	−124.2
9B−74B	17.6	−8.2
9B−79B	18.7	−14.3
9B−95A	19.1	−14.1
9B−165B[b]	19.5	−1.2
9B−82B	21.0	
9B−82A	22.7	
9B−132B	21.9	
9B−95B	25.3	
9B−147B	27.6	
9B−147A	31.9	

[a] The shortest distance between a carbon atom of the side chain of Tyr-9 in subunit B to a carbon atom of the side chain of the indicated tyrosine residue, in either subunit A or B, is reported. Some distances between Tyr-9 of subunit B and tyrosines in subunit A ae not listed because they are greater than 35 Å. Dihedral angles between aromatic rings of tyrosines within 20 Å of each other are listed.[b] Tyr-49 and Tyr-165 of human A1-1 GST are not present in the rat isozyme used in the studies reported here.

On the basis of these considerations, it is possible to obtain qualitative models for the emission spectra of Tyr-9, from difference spectra of W21F minus W21F:Y9F. The correlated 2D spectral contour of Tyr-9 at pH 7.5 is shown in Figure 4, along with the corresponding 2D surface. Note that the excitation wavelengths increase from right to left. The cross-peaks observed in the absolute excitation−emission contour of W21F (Figure 1) become dramatically more apparent when the fluorescence of other tyrosine is "subtracted". For example, the cross-peaks in the difference contour at pH 7.5 (Figure 4) are nearly equal in intensity to the cross-peaks in the absolute contour of W21F at pH 9.5 (Figure 1). Importantly, however, a significant peak remains in the difference spectra at excitation 280 nm and emission 315 nm, as expected if some of Tyr-9 is protonated. This model indicates that Tyr-9 is "heterogeneous", with properties of "normal" tyrosine as well as deprotonated or strongly hydrogen-bonded tyrosine. This result is examined in more detail in the Discussion.

In order to challenge the model provided by the "difference surface", the effects of GSH on the spectra were determined. Specifically, the results described above led to the prediction that the cross-peaks associated with the red-shifted emission should be quenched upon addition of GSH if the "difference surface" accurately reflects the properties of Tyr-9. Addition of GSH at pH 7.5 caused a nearly complete elimination of

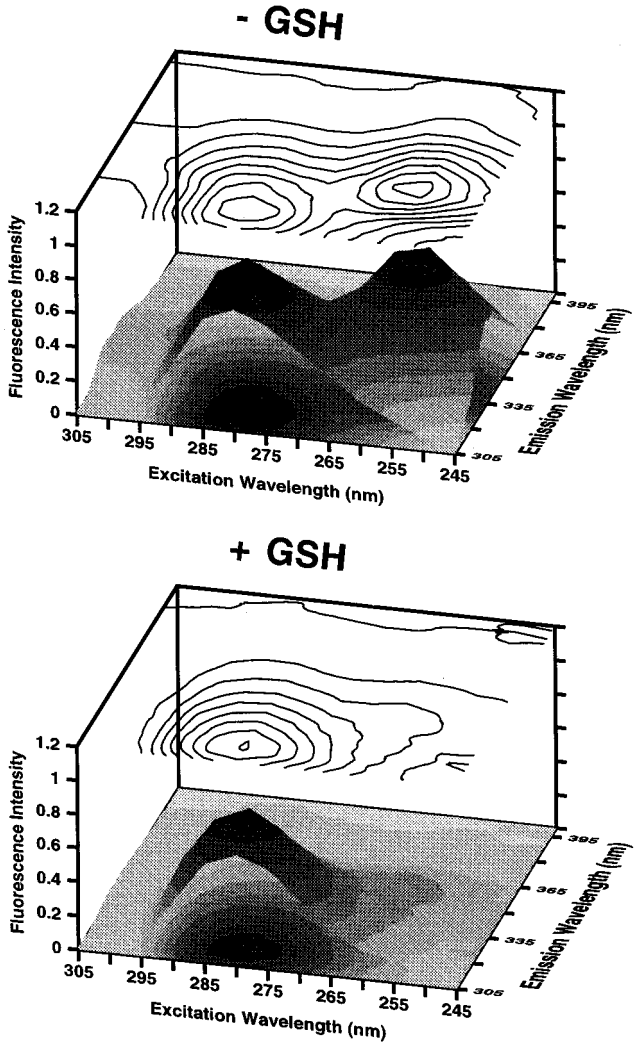

FIGURE 4: Top: Difference spectral surface of the ligand-free Tyr-9. The surface shown was obtained at pH 7.5. When the contribution from other tyrosines is subtracted, the relative spectral density at emission 340 nm, excitation 305 and 255 nm, increases compared to the absolute spectra of W21F. Bottom: Difference spectra of the GSH complex at pH 7.5. Addition of GSH quenches nearly completely the red-shifted emission component. In addition the peak intensity of the component at emission 315 nm is quenched slightly.

the cross-peaks corresponding to emission at 345 nm and excitation at 255 and 305 nm. This is consistent with the phase/modulation experiments, which indicated that the red-shifted emission component was quenched by GSH, and it further supports the qualitative accuracy of the difference spectra. Importantly, the quenching of these cross-peaks by GSH was accompanied by only a small change in the cross-peak corresponding to "normal" tyrosine, with emission at 315 nm. The peak intensity of this component is quenched by only 6%. That is, GSH quenches the fraction of Tyr-9 which has "tyrosinate" character, but GSH does not cause a spectral shift of this component to the other region of the spectrum. This is in contrast to what is observed when GSH conjugates are added (below). This result was observed also with the absolute correlated spectra of the individual W21F protein, but no spectral perturbation was observed for the absolute spectra of W21F:Y9F.

Effects of GSH Conjugates. Differential solvation of the active site in the presence of varying H-site ligands is likely to contribute to observed differences in reaction rates. Therefore, the model spectrum of Tyr-9 was used to

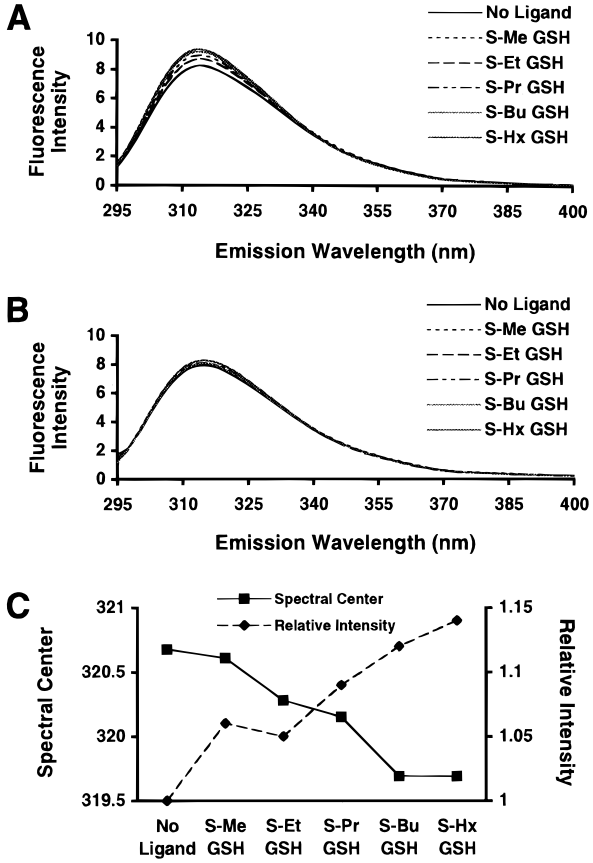

FIGURE 5: Effect of *S*-alkyl GSH conjugates on the absolute emission spectrum of W21F (A) and W21F:Y9F (B). Results shown are for pH 6.5, at which the ligand-free Tyr-9 is completely protonated. The GSH conjugates cause an increase in intensity and slight blue-shift in the spectrum of W21F. They have negligible effect on the spectrum of W21F:Y9F. Excitation wavelength was 290 nm. (C) The spectral centers of mass (nm) and peak intensities are plotted against increasing alkyl chain length of the conjugates. With larger alkyl groups, Tyr-9 becomes less solvent exposed, as indicated by the increase in intensity and shift to shorter wavelengths. *S*-Me, *S*-Et, *S*-Pr, *S*-Bu, and *S*-Hx refer to *S*-methyl, *S*-ethyl, *S*-propyl, *S*-butyl, and *S*-hexyl GSH conjugates, respectively.

determine the effects of several GSH conjugates on the active site tyrosine. In particular, Tyr-9 fluorescence provides a probe of the extent of solvation of the hydrogen bond to this residue, as well as its protonation state. As pointed out below, these GSH analogues led to a completely protonated Tyr-9, so the "base line" for comparison of GSH analogues with differing alkyl chain length should be the protonated Tyr-9 in the ligand-free GST. Therefore, the results with GSH analogues are reported for experiments at pH 6.5, where Tyr-9 is completely protonated in the ligand-free GST. Similar results were obtained at pH 7.5 and 9.5.

Two experimental probes were employed to determine the effects of GSH conjugates on the fluorescence of Tyr-9. The first was to compare directly the changes caused by ligands in the correlated spectra of W21F vs W21F:Y9F. In the first case, a series of GSH conjugates with increasing alkyl chain length was added at saturating concentration to each protein. Essentially no changes were observed in the spectrum of the W21F:Y9F mutant, whereas the W21F mutant exhibited an increase in emission intensity and a modest blue-shift in the spectral center of mass. This is most clearly evident in overlaid individual emission "slices", rather than in the correlated spectra, because the changes are relatively small (Figure 5). The spectral center of mass and peak emission

intensity are plotted vs alkyl chain length in Figure 5C. The increase in intensity and the blue-shift in the spectral center of mass with increasing alkyl chain length is directly analogous to the spectral changes that occur when tyrosines in proteins, or other phenolic fluorophores, are placed in solvents with decreasing dielectric constants or when their hydrogen-bonding partners become more anodic (Li et al., 1993; Zhao et al., 1995). These data demonstrate that, as the length of the alkyl chain of the conjugate increases, the apparent solvent accessibility of the Tyr-9 decreases (Ratacjzak, 1972; Zhao et al., 1995), assuming that each of the thioether analogues provides a hydrogen-bonding partner of similar strength. Interestingly, the *S*-methyl GSH complex yielded a spectrum which was unexpectedly like the ligand-free GST at pH 7.5 but not at pH 6.5 as shown in Figure 5C. A possible rationalization for this is provided in the Discussion.

The second approach for determining the effects of GSH conjugates on the environment of Tyr-9 was to determine the ligand-induced changes on the correlated difference surface rather than the individual absolute correlated surfaces. As described above, if other tyrosines are unaffected by these ligands, then the difference surfaces (W21F − W21F:Y9F) should reveal specific ligand-induced changes at Tyr-9. Essentially the same trend was observed, as for the individual W21F mutant. For example, the effect of *S*-hexyl GSH is demonstrated in Figure 6 (top). The red-shifted emission component is shifted to 315 nm, with a single excitation peak at 283 nm. The difference surface and the contour plot clearly demonstrate that the intensity of the peak emission at ∼315 nm increases relative to this component in the difference surface for the ligand-free Tyr-9 (Figure 4). Thus, in contrast to the effect of GSH, the *S*-alkyl analogues cause a shift of the long-wavelength spectral component to the spectral region of the other "normal" tyrosines. This component is added to the "normal" component of Tyr-9 in the difference spectrum. It is added to this component and all of the other tyrosines in the absolute spectrum of W21F. Thus, the observed affect is more dramatic with the difference spectrum than the absolute spectrum. This is true also of the blue-shift in the spectral center of mass and the peak intensity with increasing alkyl chain length, as shown in Figure 5C for the absolute spectra. That is, the total change in each of these parameters is greater for the difference spectra compared to the absolute spectra, although the changes are still modest (not shown). This provides additional support for the utility of the difference spectra as models for the spectra of Tyr-9. The difference surface, W21F − W21F:Y9F, of the complex with *S*-methyl GSH is also shown in Figure 6 (bottom). At pH 7.5 the red-shifted spectral component which is present in the ligand-free enzyme remains when *S*-methyl GSH is added at saturating concentrations. The *S*-ethyl GSH yields a complex which is nearly completely lacking this component and which is similar to the complex with *S*-hexyl GSH (not shown). Thus, at pH 7.5 the *S*-methyl complex appears "anomalous".

Information about the pK_a of Tyr-9 in the presence of these GSH conjugates is also available from these experiments. Even at pH 9.5 the spectral shift of the long-wavelength emission component which is induced by alkyl GSH conjugates is complete (not shown). Presumably, each of these ligands leads to protonation of any tyrosinate-9 which is present in the ligand-free enzyme, and a hydrogen bond is formed between the phenolic oxygen of Tyr-9 and the

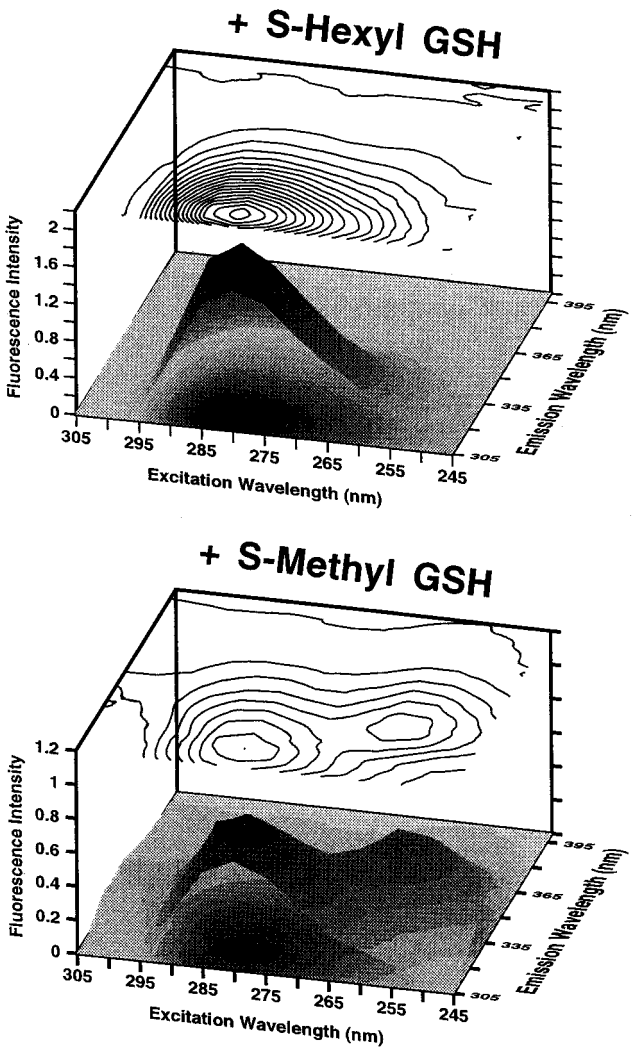

FIGURE 6: Top: Difference excitation−emission surface of the *S*-hexyl GSH complex. S-Hexyl GSH causes a spectral shift of the long-wavelength emission component of Tyr-9 to 315 nm, where it is indistinguishable from "other" tyrosines. The effect of *S*-hexyl GSH on Tyr-9 is more dramatic in the difference spectra (W21F − W21:Y9F) than in the absolute spectrum of W21F (Figure 5). A nearly 2-fold increase in intensity of the 315 nm emission component is observed, relative to the ligand-free Tyr-9, at pH 7.5. Bottom: Difference surface of the *S*-methyl complex. The red-shifted component is not quenched at pH 7.5.

thioether of the *S*-alkyl analogues. The pK_a of Tyr-9, therefore, is ≥9.5 in the presence of *S*-alkyl GSH analogues. That is, no tyrosinate component was observed in the presence of the *S*-alkyl analogues, even at pH 9.5. Above pH 9.5 other tyrosines are likely to deprotonate partially, so the pK_a of Tyr-9 has not been determined. Furthermore, the data indicate that the Tyr-9 has fluorescent properties much like other tyrosines in GST, with an emission maximum at ∼315 nm and a single broad excitation band at ∼280 nm, when it is hydrogen bonded to thioether analogues. In contrast, the hydrogen bond formed to the thiolate of GSH results in nearly complete quenching of this tyrosine, but the remaining emission is red-shifted with the excitation bands on either side of 280 nm.

In order to determine whether the spectral changes induced by GSH conjugates were due to occupation of the H-site, H-site ligands were added to the mutant proteins in the absence of GSH, and emission spectra were recorded. For example, addition of the H-site ligand 2-octenal at a concentration of 100 μM (K_i = 1.5 μM in the CDNB assay)

caused no detectable spectral change in the absolute emission spectra of W21F, W21F:Y9F, or their difference spectrum (not shown).

DISCUSSION

The environment and hydrogen-bonding characteristics of Tyr-9 of the rat A1-1 GST have been studied by a combination of steady state correlated excitation−emission spectra, time-resolved fluorescence spectroscopy, and ligand quenching experiments. An engineered rat A1-1 GST, which contains no tryptophans, and a double mutant, which also lacks the active site tyrosine, were used to generate a model of the correlated spectrum of Tyr-9. Together, the results provide a thorough spectroscopic characterization of Tyr-9, which will be useful in future experiments aimed at determining the active site residues which modulate the pK_as of Tyr-9 and bound GSH. In addition, this characterization provides the necessary data base to determine the kinetics of binding and reaction, as well as characterization of enzyme species present during steady state, for spectroscopically silent ligands. These data provide evidence also that the extent of charge transfer of the hydrogen bond to Tyr-9 changes as a function of ligand state. Presumably, the detailed structure of hydrogen bonds to Tyr-9 play a critical role in catalysis by GSTs of the alpha-, pi-, and mu-classes.

Our previous results (Atkins et al., 1993) provided spectroscopic evidence that the active site tyrosine of ligand-free cytosolic GSTs had an unusually low pK_a, as suggested by the chemical modification studies (Meyer et al., 1993) and the electrostatic calculations (Karshikoff et al., 1993). In addition, our previous results included characterization by UV−visible spectroscopy of the Tyr-9 absorption properties, which are completely consistent with the fluorescence results reported here (Atkins et al., 1993). The complete spectroscopic description of Tyr-9 provides a detailed profile of the hydrogen-bonding character of this residue in various ligand states at physiological pH.

An important finding of the fluorescence charaterization is that, in the ligand-free enzyme at pH 7.5, Tyr-9 is heterogeneous (Figure 4). A fraction of the active site Tyr-9 side chains exhibit "normal" spectroscopic properties, with an emission maximum at ∼315 nm that arises from an excitation band centered at ∼280 nm. The other fraction of Tyr-9 residues, however, clearly has absorption and emission properties which are due to either tyrosinate or strongly hydrogen-bonded tyrosine, with significant charge-transfer. Presumably, these states are in dynamic equilibrium. Due to the limitations of the difference spectra described, the fractional contribution of each state cannot be accurately determined from the difference spectra. Notably, this heterogeneity at pH 7.5 is predicted from the experimentally determined pK_a of ∼8.1, but no spectroscopic evidence has previously documented such heterogeneity for Tyr-9.

With regard to the chemical species which provides the red-shifted emission component of Tyr-9, these data can not differentiate between strongly hydrogen-bonded tyrosine, with some charge-transfer character, and formal tyrosinate. The recently published X-ray structure of the ligand-free human A1-1 GST (Cameron et al., 1995), however, indicates that no strong hydrogen bond acceptors are within 4 Å of the phenolic oxygen of Tyr-9. The amide nitrogen of Arg-15 lies within 2.8 Å and likely is a hydrogen bond donor to the oxygen atom. The other possible hydrogen bonding partner which is evident in the structure is a disordered water molecule. Typically, bulk solvent water molecules do not form hydrogen bonds with tyrosine with significant charge-transfer character (Willis & Szabo, 1991; Ratajczak, 1972). The inability of the X-ray data to clearly identify a potential strong hyrogen bond acceptor, along with the spectroscopic data presented here and elsewhere (Atkins et al., 1993; Bjornestedt, 1995), supports the possibility that a fraction of Tyr-9 is ionized as tyrosinate, at physiological pH, in the absence of ligand. Alternatively, the water molecule which is observed in the X-ray structure is "activated" to a strong base and hence to a strong hydrogen bond acceptor. It is interesting to speculate that this water molecule has hydroxide ion character, as a result of the electrostatic field provided by the side chain of Arg-15, which lies within 5.7 Å of the phenolic hydroxyl group in the apo-enzyme. It has been suggested previously that this electrostatic field stabilizes the thiolate anion of the binary complex, GS^-·GST (Bjornestedt et al., 1995). In the absence of GSH, the Arg-15 side chain does not rearrange significantly, and it may similarly stabilize the anionic hydroxide form of water, which lies between the Arg-15 side chain and the hydroxyl group of Tyr-9. This, in turn, would provide a very strong hydrogen-bonding partner which affords the "tyrosinate" species contributing to the spectrum of Tyr-9. However, if such an activated water molecule was strongly hydrogen bonded to Tyr-9, then it would be anticipated to be "well-ordered" in the X-structure. Therefore, it is likely that the red-shifted emission component observed in the ligand-free enzyme is due to tyrosinate which is present in the ground state and maintained in the excited state (Figure 7). The distinction between tyrosinate vs tyrosine which is hydrogen bonded to hydroxide may be mechanistically important, if one of these species acts as a base which directly deprotonates GSH to yield GS^- at the active site. Of course, these species may be in equilibrium with each other as well as with the protonated Tyr-9 which yields the "normal" spectroscopic component.

Addition of GSH conjugates, other than *S*-methyl GSH, leads to a hydrogen bond to Tyr-9 with much less charge transfer character than the apo-enzyme. The hydrogen bond between Tyr-9 and these alkyl GSH conjugates leads to a tyrosine which is indistinguishable spectroscopically from other tyrosines in the protein. Moreover, the data demonstrate that GSH conjugates with varying alkyl chain length differentially desolvate the immediate environment of Tyr-9. The increase in emission intensity and the concomitant blue-shift (Figure 5) are indicative of a hydrogen-bonded Tyr-9 which becomes less solvent exposed in a more hydrophobic environment as the alkyl substituent becomes longer.

The *S*-methyl GSH affords a complex with spectroscopic character like the ligand-free enzyme, at pHs above ∼7.0. Below this pH, *S*-methyl GSH causes the "expected" changes in spectral center of mass and intensity, and the spectral parameters for this complex fit the trend shown in Figure 5C. However, at higher pHs, where a significant fraction of Tyr-9 exhibits the unique spectral component, the *S*-methyl GSH complex is more like the ligand-free enzyme. This is because *S*-methyl GSH does not efficiently quench the red-shifted spectral component, which is absent at the lower pHs, as the analogues with longer alkyl chains do. That is, the *S*-methyl complex is "anomalous" at pHs which include the red-shifted spectral component but not at lower pHs where this component is absent. This interesting result indicates

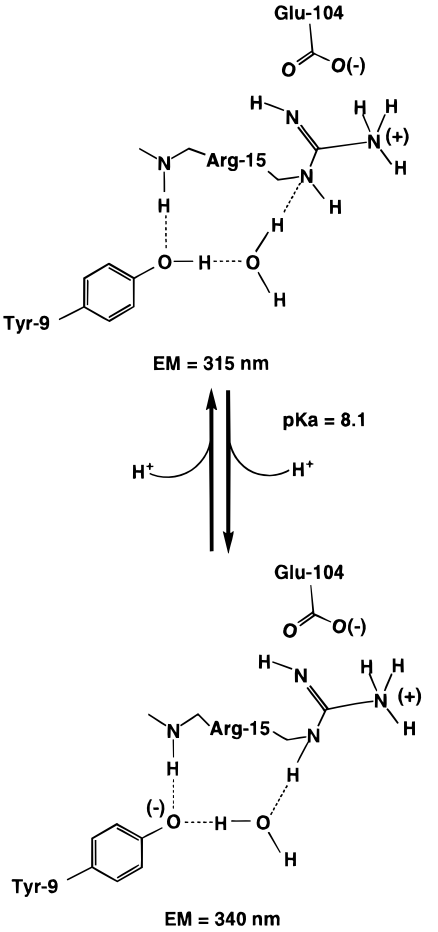

FIGURE 7: Proposed hydrogen-bonding states of Tyr-9 in the absence of ligand. The scheme is based on the X-ray structure of the ligand-free human A1-1 GST (Cameron et al., 1995). With a pK_a of ~8.1, contributions from protonated and unprotonated active sites are expected at pH 7.5. The emission component of Tyr-9 centered at 315 nm is protonated completely and hydrogen bonded to a disordered water molecule, which lies between the phenolic hydroxyl group of Tyr-9 and the side chain of Arg-15. The emission component centered at ~340 nm is likely due to formal tyrosinate hydrogen bonded to this water molecule.

that a thioether conjugate, which cannot form a strong a hydrogen bond to Tyr-9, must have a sufficiently long hydrophobic "handle" in order to displace water from the active site and hydrogen bond to Tyr-9. With only a methyl group present on the sulfur, apparently, the Tyr-9 hydrogen bonds with water rather than forming an unsolvated hydrogen bond to thioether. A bulky hydrophobic "handle" on an H-site ligand may be required to keep the Tyr-9 from being solvated by, and prevent hydrogen bonding to, water. In turn, a Tyr-9---GS^- hydrogen bond which is solvated by water is likely to result in a less nucleophilic GS^- (Huskey et al., 1991).

REFERENCES

Armstrong, R. N. (1991) *Chem. Res. Toxicol. 4*, 131−140.

Askeolf, P., Guthenberg, C. J., Jakobson, I., & Mannervik, B. (1975) *Biochem. J. 147*, 513−522.

Atkins, W. M., Wang, R. W., Bird, A. W., Newton, D. J., & Lu, A. Y. H. (1993) *J. Biol. Chem. 268*, 19188−19191.

Beaven, G. H., & Holiday, E. R. (1952) *Adv. Protein Chem. 7*, 319−386.

Beechem, J. M., Gratton, E., Ameloot, M., Knutson, J. R., & Brand, L. (1991) *Topics in Fluorescence Spectroscopy* (Lakowicz, J., Ed.) Vol. 2, pp 241−301, Plenum Press, New York.

Bjornestedt, A., Sternberg, G., Wildersten, M., Board P. G., Sinning, I., Jones, T. A., & Mannervik, B. (1995) *J. Mol. Biol. 247*, 765−773.

Cameron, A. D., Sinning, I., L'Hermite, G., Olin, B., Board, P. G., Mannervik, B., & Jones, T. A. (1995) *Structure 3*, 717−727.

Cogwill, R. W. (1976) *Biochemical Fluorescence: Concepts 2* (Chen, R. F., Edelhoch, H., Eds.) pp 441−486, Marcel Dekker, New York.

Dirr, H., Reinemer, P., & Huber, R. (1994) *Eur. J. Biochem. 220*, 645−661.

Eftink, M. (1991) *Topics in Fluorescence Spectroscopy* (Lakowicz, J., Ed.) Vol. 2, pp 53−64, Plenum Press, New York.

Eisinger, J., Feuer, B., & Lamola, A. A. (1969) *Biochemistry 8*, 3908−3915.

Graminski, G. F., Kubo, Y., & Armstrong, R. N. (1989) *Biochemistry 28*, 3562−3568.

Huskey, S.-E., Huskey, W. P., & Lu, A. Y. H. (1991) *J. Am. Chem. Soc. 113*, 2283−2290.

Ji., X., Zhang, P., Armstrong, R. N., & Gilliland, G. L. (1992) *Biochemistry 31*, 10169−10184.

Karshikoff, A., Reinemer, P., Huber, R., & Ladenstein, R. (1993) *Eur. J. Biochem. 215*, 663−670.

Ketterer, B., & Christodoulides, L. G. (1994) *Adv. Pharmacol. 27*, 37−69.

Knutson, J. R., Beechem, J. M., & Brand, L. (1983) *Chem. Phys. Lett. 102*, 2501−2507.

Kong, K.-H., Nishida, M., Inoue, H., & Takahashi, K. (1992) *Biochem. Biophys. Res. Commun. 182*, 1122−1129.

Li, Y.-K., Kuliopulos, A., Mildvan, A. S., & Talalay, P. (1993) *Biochemistry 32*, 1816−1824.

Liu, S., Zhang, P., Ji, X., Johnson, W. W., Gilliland, G. L., & Armstrong, R. N. (1992) *J. Biol. Chem. 276*, 4296−4299.

Mannervik, B., & Danielson, U. H. (1988) *Crit. Rev. Biochem. Mol. Biol. 23*, 283−337.

Meyer, D. J., Xia, C., Coles, B., Chen, H., Reinemer, P., Huber, R., & Ketterer, B. (1993) *Biochem. J. 293*, 351−356.

Ploemen, J. H. T. M., Johnson, W. W., Jersperg, S., Vanderwall, P., Van Ommen, B., van der Greef, J., van Bladderen, P. J., & Armstrong, R. N. (1994) *J. Biol. Chem. 269*, 26890−26897.

Ratajczak, H. (1972) *J. Phys. Chem. 76*, 3000−3004.

Rayner, D. M., Krajcarski, D. T., & Szabo, A. G. (1978) *Can. J. Chem. 56*, 1238−1243.

Ross, J. B. A., Laws, W. R., Rousslang, K. W., & Wyssbrod, H. R. (1992) *Topics in Fluorescence Spectroscopy* (Lakowicz, J., Ed.) Vol. 3, pp 1−54, Plenum Press, New York.

Rushmore, T. H., & Pickett, C. B. (1993) *J. Biol. Chem. 268*, 11475−11478.

Sinning, I., Kleywegt, G. J., Cowan, S. W., Reinemer, P., Dirr, H. W., Huber, R., Gilliland, G. L., Armstrong, R. N., Ji, X., Board, P. G., Olin, B., Mannervik, B., & Jones, T. A. (1993) *J. Mol. Biol. 232*, 192−212.

Wang, R. W., Pickett, C. B., & Lu, A. Y. H. (1989) *Arch. Biochem. Biophys. 269*, 536−543.

Wang, R. W., Newton, D. J., Pickett, C. B., & Lu, A. Y. H. (1991) *Arch. Biochem. Biophys. 286*, 574−578.

Wang, R. W., Newton, D. J., Huskey, S.-E., McKeever, B. M., Pickett, C. B., & Lu, A. Y. H. (1992a) *J. Biol. Chem. 267*, 19866−19871.

Wang, R. W., Newton, D. J., Pickett, C. B., & Lu, A. Y. H. (1992b) *Arch. Biochem. Biophys. 297*, 86−91.

Wang, R. W., Bird, A. W., Newton, D. J., Lu, A. Y. H., & Atkins, W. M. (1993) *Protein Sci. 2*, 2085−2094.

Wetlaufer, D. B. (1962) *Adv. Prot. Chem. 17*, 303−390.

Willis, K. J., & Szabo, A. G. (1991) *J. Phys. Chem. 95*, 1585−1589.

Wu, P., Li, Y.-K., Talalay, P., & Brand, L. (1994) *Biochemistry 33*, 7415−7422.

Zhao, Q., Mildvan A. S., & Talalay, P. (1995) *Biochemistry 34*, 426−434.

BI9530346